Effects of Calibration RFID Tags on performance of Inertial Navigation in Indoor Environment

Guanxiong Liu, *Student Member, IEEE,* Yishuang Geng, *Student Member, IEEE*
Kaveh Pahlavan, *Fellow, IEEE,*
Center for Wireless Information Network Studies, Worcester Polytechnic Institute, Worcester, MA 01609 USA
Email: {gliu2, ygeng and kaveh}@wpi.edu

***Abstract*—The hybrid localization system applications nowadays not only mitigate the inaccuracy of standalone RF localization approach, but also increase the reliability in the absence of supporting Radio Frequency (RF) infrastructure. One of the outstanding hybrid approaches is the Radio Frequency Identification(RFID) assisted inertial navigation system, which is notable for its low cost, simple implementation and extraordinary accuracy. Previous work on such hybrid system fails to find out the correlation between the deployment of the multiple calibration points and the indoor localization accuracy. In this paper, we use the Android smart phone to build a hybrid localization platform and conduct measurements with multiple RFID calibration tags. Based on the measurement results, we define a mathematical model which includes the calibration point number, RFID tag density and the RFID tag-to-corner distance to describe the deployment effect on the localization accuracy. Such model facilitates the future study on algorithm design, system evaluation and application development.**

***Keywords*—Radio frequency identification (RFID), inertial navigation system (INS), calibration, deployment, modeling**

I. Introduction

Nowadays, the rapid advancement of wireless access and localization technology not only provides high data rate wireless communication, but also realizes the precise indoor localization [1]. With the well known received signal strength (RSS), time-of-arrival (TOA), angle-of-arrival (AOA) based approaches, location information can be obtained even in the indoor area that global positioning system (GPS) could never cover. Since wireless indoor localization requires the prior knowledge of the reference points and suffers from the multipath phenomenon caused by complicated indoor environment, the traditional pedestrian dead reckoning method maintains its priority in the absence of supporting infrastructure [2] [3]. To further improve the localization accuracy for critical cases such as localizing patients, prisoners and first responders, research campaign proposed cooperative localization applications to combine multiple approaches [4] [5].

Among all available hybrid localization technologies, RFID assisted approach is always under the limelight for its low energy consumption, low cost characteristic and simple implementation. With the concept of smart building widely spread, the trend of using RFID tag in cooperative localization get further promoted to the maximum. Ni et al. proposed 'LANDMARK', the first prototype system using active RFID technology to obtain location information in indoor environment [6]. More recently, Ruiz et al. reported a pedestrian navigation system using tightly coupled foot-mounted IMU and RFID ranging to achieve accurate indoor localization [7]. These applications utilize RFID tag as transceivers and require ranging process. Apart from that, other researches regard the RFID tag as a calibration point with small enough coverage that serve as a landmark for pass-by objects. Such works include the RFID-assisted localization system for first responders [8] [9]; Self-calibrated RFID tags in smart factory [10] and even location estimation system for construction materials [11]. Note that in this work, we focus on the second category of RFID assisted indoor localization and employ the RFID tag for calibration purpose only.

The above mentioned works in the open literature generally focused on system implementation, algorithm optimization, robustness to multipath and etc., however, they merely looked into the influence of RFID tag number or geometrical deployment of the tags. Ruiz et al. graphically illustrated the effect of tag numbers but failed to quantitatively model it [7]; Hameed et al. tried to sparsely distribute the tags in the smart factory and evaluated multiple deployment topology but did not report any mathematical model regarding tag location [10]. Although it is intuitive that avoiding linearly-aligned, close-range calibration tags may help getting better dilusion of position (DOP) [12], yet an optimized way of tag deployment is still essential and urgently demanded for both academic and industry.

In this paper, the performance of RFID assisted inertial navigation system has been measured in a typical office environment with different number of calibration RFID tags and various combination of tag locations. Based on the empirical data, the effect of calibration tag number and tag locations have been investigated. In order to quantitatively describe these effects, mathematical model for average localization error has been built using tag number, tag-to-corner distance and tag density as parameters. The proposed model can be uniformly used in general scenario given floor layout, which may benefit future tag deployment optimization and system performance evaluation to a large scale.

The remainder of this paper is organized as follows. In section II, the measurement scenario and measurement system has been introduced and necessary definitions has been provided for further analysis. In section III, the effect of tag deployment has been analyzed from the perspective of calibration tag number, tag-to-corner distance and tag density. In section IV, regression fitting has been applied to empirical data and

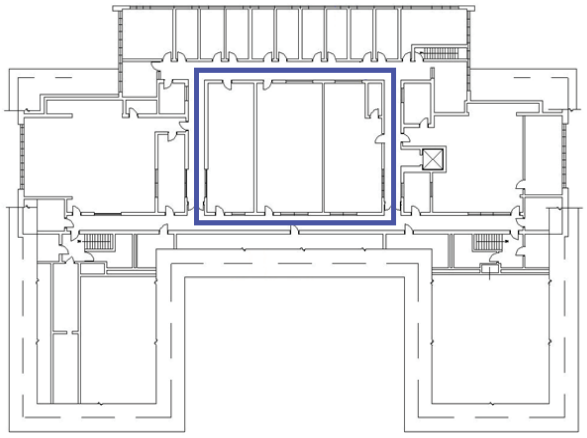

Fig. 1. 2D floor layout for Atwater Kent building, WPI.

mathematical model has been built to illustrate the influence of tag deployment on localization accuracy. In section V, we summarize this paper and discuss future work.

II. Scenario and System Setup

In this section, the measurement scenario, system setup as well as necessary parameter definitions have been discussed. We conducted on-line measurement for pedestrians dead reckoning (PDR) indoor navigation in a typical office floor and the assistance of RFID calibration tags is achieved by off-line software simulation. Since this work focus on small range calibration tags with directional antenna, we assume that the RFID calibration has a 0.1m accuracy so that the calibration process can be simplified as moving the PDR particle with state $(\hat{x}_i, \hat{y}_i, \hat{\theta}_i)$ back to a random location within 0.1m radius to the calibration tag location. For PDR measurements, $\hat{x}_i$, $\hat{y}_i$ denotes to the coordinate estimate for i^{th} particle and $\hat{\theta}_i$ denotes to the heading.

A. Measurement Scenario

On-line measurement for PDR navigation is performed at the 3rd floor of the Atwater Kent Laboratory, the office building of ECE department, Worcester Polytechnic Institute, Worcester, MA, USA. As shown in Fig. 1, there is a rectangular path along the main corridor of $27.6 \times 20.4m$. The objective first and foremost goes through a training process to obtain the average step length l and then walks along the main corridor on a constant speed, holding the smart phone in hand. The measurement starts from the bottom left corner of the path and lasts for three entire cycles. Note that constant walking model is not a limitation on this work, preliminary results shows that following discussion still applied to random walking situation and it will be mentioned in future publications.

B. System Setup

The entire measurement process is performed using a self-designed android application on Samsung Exhibit II SGH-T679 smart phone, which runs on any android system above version 2.2 and is embedded with accelerometer and compass for step detection and heading measurement respectively. Every time a step is detected, a PDR particle is recorded in the format of $(\hat{x}_i, \hat{y}_i, \hat{\theta}_i)$ based on coordinate and heading measurement on previous step. The update process of particles can be given as

$$\hat{x}_{i+\delta i} = \hat{x}_i + (l + n_l)\cos(\delta\hat{\theta} + n_\theta) \tag{1}$$

$$\hat{y}_{i+\delta i} = \hat{y}_i + (l + n_l)\sin(\delta\hat{\theta} + n_\theta) \tag{2}$$

$$\hat{\theta}_{i+\delta i} = \hat{\theta}_i + \delta\hat{\theta} + n_\theta \tag{3}$$

where δi is the step counts from the last known particle, $\delta\hat{\theta}$ denotes the the heading change, n_l and n_θ are noise terms drawn from the step length and heading uncertainty models respectively. The iterative process indicates that the beginning state is required for this approach. Note that due to the metallic structure of the building and dense RF devices in some of the rooms, the heading measurement could be erroneous. Inaccuracy on steps length is also possible since the training performance is limited to some scale. To represent the above mentioned uncertainty, the localization error for specific PDR particle is defined as

$$\epsilon_i(d) = \sqrt{(\hat{x}_i - x_i)^2 + (\hat{y}_i - y_i)^2} \tag{4}$$

where x_i, y_i are the ground true coordinate for i^{th} PDR particle.

C. Parameter Definitions

Apart from the state information of PDR particles, calibration tag locations is also recorded during our experiments. RFID tags are by nature attached to the walls and very frequently appears close to corridor corners for the sake of convenience and aesthetics. Also, the ultimate goal is to track objectives in the public area instead of private room. We consider RFID tags deployed along the path in the main corridor. The candidate set for calibration point number in this work can be given by $m \in \mathcal{M} = \{1, 2, ..., M\}$ where m denotes the index of m^{th} RFID calibration tag and $M = 8$ in this work. Since dramatic heading change can be detected at the corners along the path, tags attached to the corner may intuitively limited the inaccuracy caused by heading measurement. To represent how far are the calibration tags located from the corners, we define the tag-to-corner distance d_{corner} as the average of distances between each tag and its nearest corner on the floor layout, which can be given as

$$d_{\text{corner}} = \frac{1}{M}\sum_{m\in\mathcal{M}}[\min_{j\in\mathcal{J}}(\sqrt{(x_m - x_j)^2 + (y_m - y_j)^2})] \tag{5}$$

where x_m, y_m are the coordinate for m^{th} RFID calibration tag and x_j, y_j are the coordinate for j^{th} corner. In this specific measurement scenario, candidate set for corner index is $j \in \mathcal{J} = \{1, 2, 3, 4\}$. Moreover, to represent the influence of homogeneous density of tag deployment, we define tag density

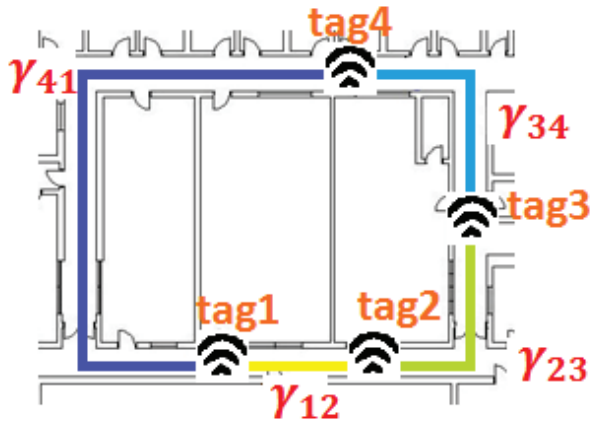

Fig. 2. Sample calibration tag deployment when $n = 4$.

d_{dense} as the average of distance between adjacent tags, which is given by

$$d_{\text{dense}} = \frac{1}{M-1}[\mathcal{P} - \max_{m \in \mathcal{M}}(\gamma_{m,m+1_{\text{Mod}(M)}})] \tag{6}$$

where $\mathcal{P}$ is the total length of the target trajectory, which is along the rectangular path in this work, $\gamma_{m,m+1_{\text{Mod}(M)}}$ denotes the distance between adjacent tags along trajectory and is given as

$$\gamma_{m,m+1_{\text{Mod}(M)}} = \int_{C_{m,m+1}} fds = \int_{\text{tag}_m}^{\text{tag}_{m+1_{\text{Mod}(M)}}} f(r(t))|r'(t)|dt \tag{7}$$

where $C_{m,m+1}$ is the trajectory between m^{th} and $m+1^{th}$ calibration tag, f is the scaler field and is constant 1 for 2D case, $\text{tag}_m = (x_m, y_m)$ denotes the coordinate for m^{th} calibration tag, $r(t)$ represents the sample point for line integral. Since we have to take the $\gamma_{M,1}$ into consideration in the $\max(\bullet)$ operation in (6), Mod(M) calculation has been included. Typical test case has been illustrate in Fig. 2, in which the tag number and distance between adjacent tags has been specified. Note that the density employed in this paper is a linear density instead of spatial density due to the fact that the ultimate goal is to track objectives in the public area instead of private room. It is worth mentioning that with the priori knowledge of floor layout, the line integral can be easily simplified into summation of distance along the trajectory, reducing the computational complexity to the minimum.

Based on the pre-defined parameters, with given calibration tag deployment, the localization error for specific target position can be defined as

$$\epsilon_{n,d_{\text{corner}},d_{\text{dense}}} = \sqrt{(\hat{x}_{n,d_{\text{corner}},d_{\text{dense}}} - x)^2 + (\hat{y}_{n,d_{\text{corner}},d_{\text{dense}}} - y)^2} \tag{8}$$

where $\hat{x}_{n,d_{\text{corner}},d_{\text{dense}}}$, $\hat{y}_{n,d_{\text{corner}},d_{\text{dense}}}$ denote to the location estimate given specific calibration tag number and tag deployment. Throughout the off-line software simulation for various tag locations, we include all possible combination of n, d_{corner} and d_{dense}.

III. Effect of Tag Number, Tag-to-Corner Distance and Tag Density

General localization error for the RFID assisted inertial navigation system has been plotted in Fig. 3 and Fig. 4. In Fig. 3, with no calibration, it is very obvious that localization result keeps drifting away from the ground truth. Such drifting phenomenon agree with the pure PDR system performance bound reported in previous works. When RFID calibration tag gets involved, localization performance gets improved to a large degree and the drifted result is pulled back to ground truth even though the uncertainty still exists. Conclusion can

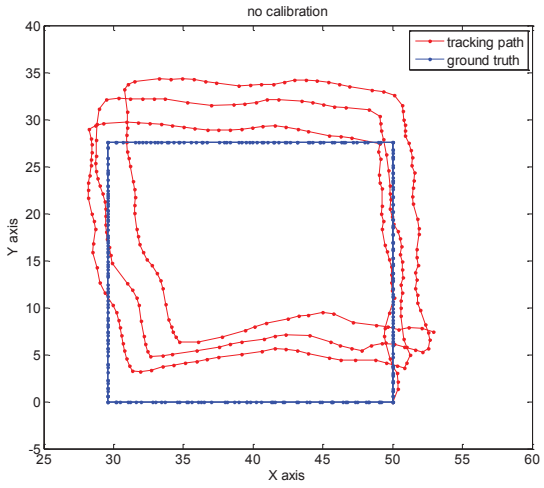

Fig. 3. Empirical result for pure PDR navigation without RFID calibration points.

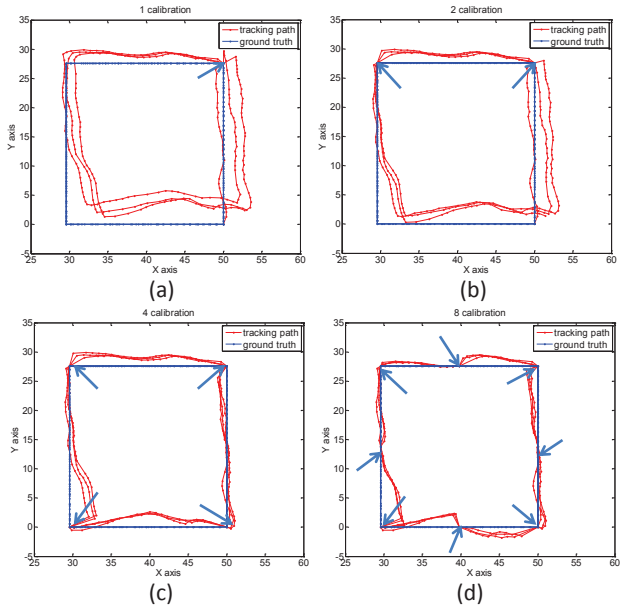

Fig. 4. Empirical result with RFID assisted multiple calibration. (a) $n = 1$; (b) $n = 2$; (c) $n = 4$; (d) $n = 8$.

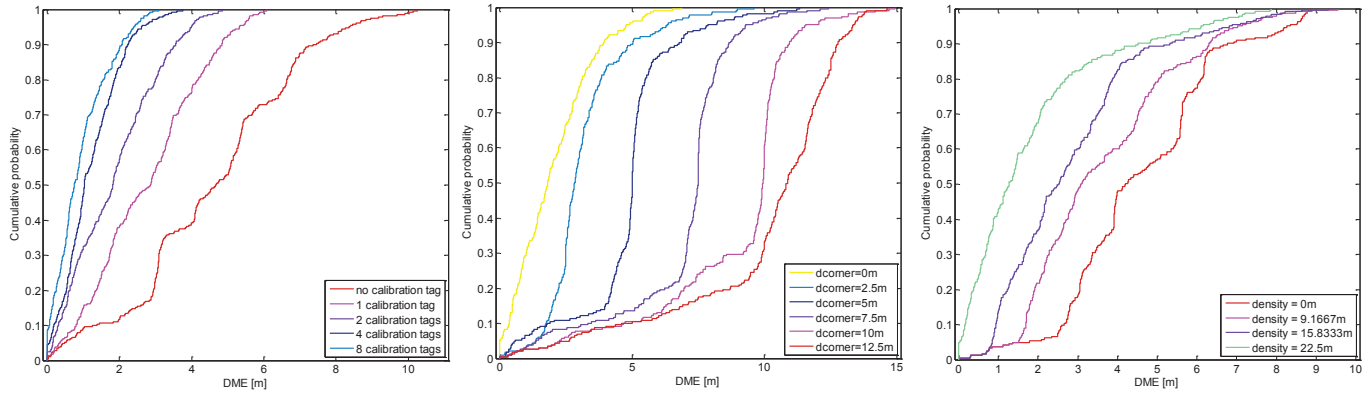

(a) (b) (c)

Fig. 5. CDF plot for the effect of tag number and tag locations. (a) Effect of calibration tag number; (b) Effect of calibration tag-to-corner distance; (c) Effect of calibration tag density.

be drawn from Fig. 4 is that with the increment of calibration point number, localization accuracy becomes better. To better illustrate the statistics of the empirical result, cumulative density function of $\overline{\epsilon}_{n,d_{\text{corner}},d_{\text{dense}}}$ for localization accuracy with different number of calibration tags has been depicted in Fig. 5(a), from which we can see that for a given floor layout, a sufficient number of calibration tag can be implied. If the tag number is more than adequate, the extra tags have very limited contribution on the performance improvement. In this work, sufficient number would be 4 tags. When using 8 tags to calibrate the PDR system, performance improvement is highly limited.

As for the influence of tag-to-corner distance, the experimental result shows that RFID calibration tags in the corner contribute more on the improvement of localization performance. Statistic for the effect of tag-to-corner distance has been illustrated in Fig. 5(b), in which the CDF for $\overline{\epsilon}_{n,d_{\text{corner}},d_{\text{dense}}}$ has been plotted with four calibration tags, same tag density but various tag-to-corner distance. Identical tag density can be guaranteed by initiate the four calibration tags at the four corner and step by step move the tags along same direction. As long as the step size is constant, tag density will not change. Statistics show that with the increment of d_{corner}, localization error becomes larger, indicating that it is preferred to deploy calibration tags as close to corners as possible.

The effects of tag density can not be ignored since in most of the previous work of INS with multiple calibration, people always tried to figure out a way to uniformly deploy the calibration points. Four tag calibration case has been again plotted in Fig. 5(c) with fixed tag-to-corner distance and various tag density. It shows that with uniformly deployed calibration tags, best localization performance can be achieved. The integrated analysis on the effect of tag number and tag locations propose a tough question on the optimized deployment, that is, how can we manage the trade-off among tag number, tag-to-corner distance and tag density. To answer that question, we proposed a mathematical model to support deployment optimization.

IV. Modeling the Effect of Tag Deployment

To quantitatively describe the trade-off among n, d_{corner} and d_{dense}, mathematical model on localization error has been proposed in this section. The empirical data shows that localization error $\epsilon_i(d)$ can be modeled as a uniformly distributed random variable and as long as we have at least one calibration point, the variance of $\epsilon_i(d)$ is limited in a small range. Based on that observation, we focus on the average localization error $\overline{\epsilon}_{n,d_{\text{corner}},d_{\text{dense}}}$ and do not take the variance into consideration. By further examining the empirical measurement results, we notice that for a given n and d_{corner}, linear relationship between $\overline{\epsilon}_{n,d_{\text{corner}},d_{\text{dense}}}$ and d_{dense} can be obtained as

$$\overline{\epsilon}_{n,d_{\text{corner}},d_{\text{dense}}} = A_{n,d_{\text{corner}}} \times d_{\text{dense}} + B_{n,d_{\text{corner}}} \tag{9}$$

where $A_{n,d_{\text{corner}}}$ and $B_{n,d_{\text{corner}}}$ are intermediate coefficients depends on calibration number n and tag-to-corner distance d_{corner}. Case specific fitting result for $\overline{\epsilon}_{n,d_{\text{corner}},d_{\text{dense}}}$ has been plotted in Fig. 6(a) in which four calibration tags are employed. Exploiting $A_{n,d_{\text{corner}}}$ and $B_{n,d_{\text{corner}}}$ for different calibration tag number, we can further model the relationship between intermediate coefficients and tag-to-corner distance as

$$\begin{cases} A_{n,d_{\text{corner}}} = C_n \times d_{\text{corner}} + D_n \\ B_{n,d_{\text{corner}}} = B_{d_{\text{corner}}} = E \times d_{\text{corner}} + F \end{cases} \tag{10}$$

TABLE I. Coefficients for the Proposed Model.

n	C_n	D_n	E	F
2	0.00187	-0.02493		
3	0.00374	-0.06587		
4	0.00603	-0.1140		
5	0.00709	-0.1586	-0.0821	4.541
6	0.00902	-0.2044		
7	0.01001	-0.2458		
8	0.01174	-0.2942		

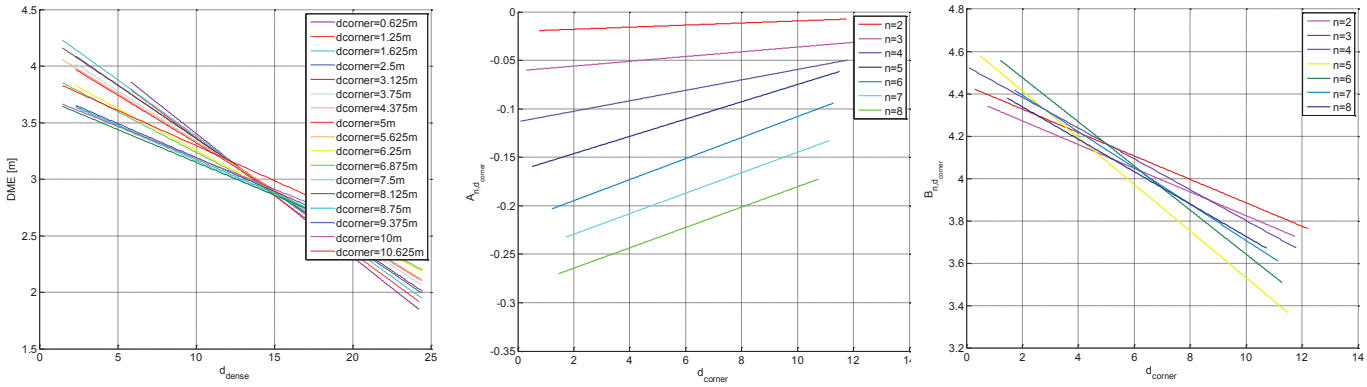

(a) (b) (c)

Fig. 6. Regression fitting result. (a) $\bar{\epsilon}_{n,d_{\text{corner}},d_{\text{dense}}}$ vs. d_{dense}; (b) $A_{n,d_{\text{corner}}}$ vs. d_{corner}; (c) $B_{n,d_{\text{corner}}}$ vs. d_{corner};

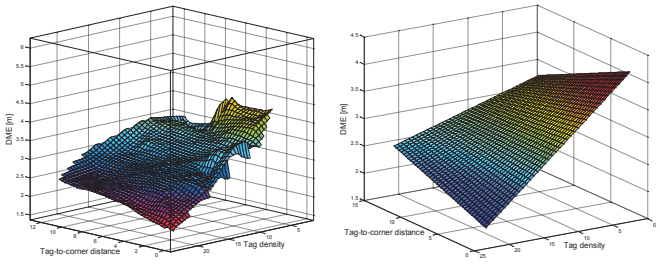

(a) Empirical data. (b) Proposed Model

Fig. 7. Validation for the proposed model.

where C_n and D_n are coefficients depends on tag number n, E and F are constant coefficients. We could further fit C_n and D_n by n, however, since the tag number could be integers only and massive curve fitting influences the accuracy of error model, Table. I has been provided for C_n and D_n regarding different tag number n. Fitting result for $A_{n,d_{\text{corner}}}$ and $B_{n,d_{\text{corner}}}$ have been depicted in Fig. 6(b) and (c) respectively and the final model for averaging localization error can be given as

$$\begin{aligned}\bar{\epsilon}_{n,d_{\text{corner}},d_{\text{dense}}} &= (C_n \times d_{\text{corner}} + D_n) \times d_{\text{dense}} + E \times d_{\text{corner}} + F \\ &= C_n \times d_{\text{corner}} \times d_{\text{dense}} + D_n \times d_{\text{dense}} + E \times d_{\text{corner}} + F\end{aligned} \tag{11}$$

where C_n, D_n, E and F can be found in Table. I. To further validate the proposed average localization error model, we select typical measurement cases and compare it with the software simulated localization error model. As shown in Fig. 7, given $n = 4$, the empirical measurement result in Fig.7(a) has a highly agreement with simulated error model in Fig. 7(b), which further prove the validity of the proposed average localization error model.

V. Conclusion

The major contribution of this paper is that we analyzed the effect of calibration tag number, tag-to-corner distance and tag density on average localization error for the RFID assisted inertial navigation system with multiple calibration. Mathematical model has been proposed for deployment optimization and it also facilitates the future study on algorithm design, system evaluation and application development.

References

[1] J. He, Y. Geng, Y. Wan, S. Li, and K. Pahlavan, "A cyber physical testbed for virtualization of rf access environment for body sensor network," *Sensor Journal*, vol. 13, no. 10, pp. 3826–3836, 2013.

[2] J. Bird and D. Arden, "Indoor navigation with foot-mounted strapdown inertial navigation and magnetic sensors [emerging opportunities for localization and tracking]," *Wireless Communications, IEEE*, vol. 18, no. 2, pp. 28–35, 2011.

[3] Y. Geng, H. Deng *et al.*, "Modeling the effect of human body on toa ranging for indoor human tracking with wrist mounted sensor," in *Wireless Personal Multimedia Communications (WPMC), 2013 16th International Symposium on*. IEEE, 2013, pp. 1–6.

[4] R. W. Ouyang, A.-S. Wong, and C.-T. Lea, "Received signal strength-based wireless localization via semidefinite programming: noncooperative and cooperative schemes," *Vehicular Technology, IEEE Transactions on*, vol. 59, no. 3, pp. 1307–1318, 2010.

[5] Y. Ma, L. Zhou, K. Liu, and J. Wang, "Iterative phase reconstruction and weighted localization algorithm for indoor rfid-based localization in nlos environment," *Sensor Journal, IEEE*, vol. 14, no. 2, pp. 597–611, 2014.

[6] L. M. Ni, Y. Liu, Y. C. Lau, and A. P. Patil, "Landmarc: indoor location sensing using active rfid," *Wireless networks*, vol. 10, no. 6, pp. 701–710, 2004.

[7] A. R. J. Ruiz, F. S. Granja, J. C. Prieto Honorato, and J. I. G. Rosas, "Accurate pedestrian indoor navigation by tightly coupling foot-mounted imu and rfid measurements," *Instrumentation and Measurement, IEEE Transactions on*, vol. 61, no. 1, pp. 178–189, 2012.

[8] J. Guerrieri, M. Francis, P. Wilson, T. Kos, L. Miller, N. Bryner, D. Stroup, and L. Klein-Berndt, "Rfid-assisted indoor localization and communication for first responders," in *Antennas and Propagation, 2006. EuCAP 2006. First European Conference on*. IEEE, 2006, pp. 1–6.

[9] Y. Geng, J. Chen, and K. Pahlavan, "Motion detection using rf signals for the first responder in emergency operations: A phaser project," in *Personal Indoor and Mobile Radio Communications (PIMRC), 2013 IEEE 24th International Symposium on*. IEEE, 2013, pp. 358–364.

[10] B. Hameed, F. Rashid, F. Dürr, and K. Rothermel, "Self-calibration of rfid reader probabilities in a smart real-time factory," in *Pervasive Computing*. Springer, 2012, pp. 253–270.

[11] S. N. Razavi and C. T. Haas, "Using reference rfid tags for calibrating the estimated locations of construction materials," *Automation in Construction*, vol. 20, no. 6, pp. 677–685, 2011.

[12] I. Sharp, K. Yu, and M. Hedley, "On the gdop and accuracy for indoor positioning," *Aerospace and Electronic Systems, IEEE Transactions on*, vol. 48, no. 3, pp. 2032–2051, 2012.